Does litter input determine carbon storage and peat organic chemistry in tropical peatlands?

Abbie Upton[1], Christopher H. Vane[2], Nick Girkin[1], Benjamin L Turner[3] and Sofie Sjögersten[1*].

[1]The University of Nottingham, School of Biosciences, Division of Agricultural and Environmental Science, Sutton Bonington Campus, Loughborough, LE12 5RD, UK

[2]British Geological Survey, Organic Geochemistry, Centre for Environmental Geochemistry, Keyworth, Nottingham NG12 5GG, UK

[3]Smithsonian Tropical Research Institute, Apartado 0843-03092, Balboa, Ancon, Panamá, Republic of Panama

Abstract

Tropical peatlands hold large amounts of carbon but the influence of litter inputs and variation in peat properties with depth on carbon storage are poorly understood. Here we present a stratigraphy of peatland carbon stocks and accumulation through the peat profile in a tropical ombrotrophic wetland and assess shifts in vegetation inputs and organic matter degradation using *n*-alkane distributions and Rock-Eval 6 pyrolysis. Mixed forest (including canopy palms and tropical hardwood trees) contained the greatest total carbon stock in the soil (1884 Mg C ha^{-1}), followed by *Rhizophora mangle* (mangrove, 1771 Mg C ha^{-1}), *Campnosperma panamensis*

(hardwood, 1694 Mg C ha^{-1}) and *Cyperus* (sawgrass) bog plain (1488 Mg C ha^{-1}). The long-term apparent rate of carbon accumulation, determined by ^{14}C dating of the carbon stored in different layers in the peat profile, decreased from the edge to the interior of the peatland, with the highest accumulation rate in at the *Rhizophora* site (102.2 g C m^{-2} y^{-1}) and the lowest in the deeper peat layers at the *Cyperus* site (45.6 g C m^{-2} y^{-1}). High molecular weight *n*-alkanes dominated in surface peat in all four phasic communities, while deeper in the peat profile *n*-alkane profiles differed more among sites, suggesting contrasting litter inputs (e.g. shifts from terrestrial vegetation to aquatic inputs) or decomposition environments. Deeper peat was depleted in carbohydrates and had a relatively larger thermostable C pool. Taken together our findings show (i) that different forest types hold varying C stocks and have different peat accumulation rates, even over relatively small distances, and (ii) progressive depletion of carbohydrates and thermolabile compounds with depth, despite strong variation in litter inputs throughout the peat profile.

Keywords: Carbon storage, decomposition, tropical peatland, Rock-Eval pyrolysis, *n*-alkanes, FTIR.

1 Introduction

Global peatlands account for approximately 3% of the Earth's terrestrial area, of which 10% are situated within the tropics (Chimner and Ewel, 2005). Tropical peatlands consist of partially decomposed organic matter, which has accumulated under waterlogged, anaerobic conditions, typically over millennia, when vegetation input exceeds decomposition (Andriesse, 1988; Minasny et al., 2016; Wösten et al., 2008; Sjögersten et al., 2014; Hoyos-Santillan et al., 2015). Globally, peatlands are estimated to store 105 Gt C, equivalent to ca 20% of the Earth's peatland carbon store (Jaenicke et al., 2008; Page et al., 2011; Dargie et al., 2017). However, over the last century the sink strength of tropical peatlands has been under threat from logging, drainage and fires, particularly in areas of increasing population growth and development (Chimner and Ewel, 2005; Hooijer et al., 2010; Limpens et al., 2008; Wösten et al., 2008). Climate change also has an impact on the functioning of tropical peatlands, due to changes in precipitation, which lead to increased risk of drought (Chimner and Ewel, 2005; Page et al., 2011). These changes alter vegetation inputs and organic decomposition rates, and increase the risk of peatlands becoming carbon sources (Wösten et al., 2008).

Many tropical peatlands demonstrate a lateral sequence of vegetation types or phasic communities (Anderson, 1964; Page et al., 1999; Phillips et al., 1997). For example, a paleoecological study by Phillips et al. (1997) revealed spatial variation in the dominant peat-forming vegetation from the edge to the interior of a large domed coastal swamp in Panama. Surface vegetation type is a major control on peat properties, as it determines the quantity and quality of litter, which contributes to the peatland organic matter (Laiho, 2006; Sjögersten et al., 2011; Ward et al., 2015). In tropical peatlands, litter containing high concentrations of carbohydrates, the rate of

decomposition is relatively fast, compared to lignin-rich litter (Hoyos-Santillan et al., 2015). Therefore, vegetation type controls, in part, the rate of carbon accumulation in tropical peatlands, causing variations spatially and with depth (Limpens et al., 2008; Sjögersten et al., 2011). It is therefore important to determine how phasic communities differ with regard to initial transformation of the litter input as it become incorporated into the peat, and total carbon stocks through the peat profile.

Litter decomposition alters the organic matter chemistry over time with different litter species and tissue types degrading at different rates (Wright et al., 2013; Hoyos-Santillan et al., 2015; Vane et al., 2013). Furthermore, decomposition alters peat physical properties resulting in denser, less porous peats (Tuat et al., 2011; Tonks et al., 2017; Brain et al., 2017). Indeed, changes in bulk density are important in controlling carbon storage, which often varies throughout peatlands (Warren et al., 2012; Tonks et al., 2017). However, despite the importance of litter inputs and subsequent decomposition for carbon storage in tropical peatlands (Sjögersten et al., 2014), the long term fate of litter inputs remain poorly understood. A key knowledge gap hampering our understanding of peat accumulation in tropical wetlands is how carbon accumulation is affected by variation in litter inputs and decomposition due to differences in successional vegetation communities.

Spatial and depth variation in the physical properties and biogeochemistry of organic matter corresponding to shifts in phasic communities within the San San Pond Sak peatland in Panama have been reported by Cohen et al. (1989), Phillips et al. (1997), Sjögersten et al. (2011), Wright et al. (2011) and Cheesman et al. (2012). Therefore, we used the San San Pond Sak peatland to assess how carbon storage capacity and peat organic chemistry was linked to shifting vegetation inputs and decomposition through the peat profile. In this study, we present a stratigraphy of

peatland physical properties and an assessment of the degree of decomposition in four common distinct vegetation communities within the San San Pond Sak peatland. Specifically, we determined carbon stocks and accumulation rates through the peat profiles, to assess shifts in vegetation inputs and organic matter degradation we analysed peat profile *n*-alkane distributions while Rock-Eval 6 pyrolysis was used to develop high resolution depth profiles of the peat thermal stability, which is linked to its organic matter composition. Rock-Eval 6 pyrolysis has been used to investigate carbon dynamics within a range of systems e.g. mangrove (Marchand et al., 2008), marine sediments (Hare et al., 2014), freshwater and saltmarsh peats (Engelhart et al., 2013 Newell et al., 2016; Kemp et al., 2017), as well as trends in SOM dynamics through soil profiles (Sebag et al., 2006, Delarue et al., 2013; Biester et al., 2014; Sebag et al., 2016), providing a powerful tool for rapid assessment of shifts in peat organic geochemistry among vegetation types and depth.

We used the data to test the following hypotheses: (1) long-term rates of carbon accumulation (LORCA) vary spatially across the vegetation gradient; (2) surface peat is dominated by long chain *n*-alkanes while deeper peat contain more mid chain length n-alkanes reflecting decay of vegetation inputs; (3) increased peat degradation with depth will result in depletion of carbohydrates relative to aromatics overriding variation in litter inputs due to successional changes in the vegetation and hence litter inputs over time (Phillips et al., 1997); (4) the thermal stability of the peat is related to litter input and increases with depth as the peat become more degraded.

2 Methods

2.1 Study Site and Sampling

The San San Pond Sak peatland is located in the Bocas del Toro Province on the coast of western Panama (Wright et al., 2011). The area contains a mixture of freshwater and marine influenced wetlands and includes the Changuinola peat deposit, which is estimated to have formed up to 4000 years ago (Phillips et al., 1997). Seven distinct phasic communities have been identified across the peatland, in roughly concentric rings (Phillips et al., 1997). Starting from the periphery, these communities have been designated as (i) *Rhizophora mangle* mangrove swamp, (ii) mixed back mangrove swamp, (iii) *Raphia taedigera* palm forest swamp, (iv) mixed forest swamp (consisting of both palm and evergreen broadleaved hardwood trees), (v) *Campnosperma panamensis* forest swamp, (vi) sawgrass/stunted forest swamp and (vii) *Myrica-Cyrilla* bog-plain. In this study we focused on (i), (iv), (v) and (vi) of these phasic communities to traverse the full range of successional stages and also as these were the main communities identified along a transect from the coast to the centre of a secondary peat dome to the east of the main peat dome. The species composition of the phasic communities and soil properties are detailed in Phillips et al., (1997) and Sjogersten et al., (2011 and 2018). Briefly, the mangrove site is dominated by *Rhizophora mangle*; the mixed forest is the most diverse sites with regards to tree species with the most common being *C. panamensis, Euterpe precatoria, Symphonia globulifera, R. taedigera, Chamaedorea pauciflora, Cassipourea elliptica*; the *Campnosperma panamensis* forest swamp is monodominant (i.e. >80% of the trees are *C. panamensis*); the bog-plain was tree-less and vegetated by *Cyperus* species. The mean annual precipitation of the area is 3092 ± 181 mm, and the mean annual air temperature in the area is 25.9 ± 0.3 °C

(Hoyos-Santillan et al., 2015). There is no distinct seasonality in the region, the water table remains close to the surface of the peatland throughout the year (range is -40 to +40 cm during shorter periods of drought and high rainfall). At the central areas (phasic community IIV) of the peatland track tracks are flooded for a large part of the year. There are two distinct periods of lower rainfall in February-April and September-October (Hoyos-Santillan et al., 2015; Wright et al., 2011).

Study sites were established across a transect of a small dome to the east of the main deposit. The sites are shown in Figure 1 and were located within four of the main phasic communities as described by Phillips et al. (1997).

At these sites, peat cores of 50 cm length were collected down to 630 cm for *Rhizophora*, 510 cm for mixed forest, 529 cm for *Campnosperma* and 530 cm for Cyperus using the same method to that described in Nikitina et al. (2014) and Vane et al. (2013). Upon collection cores were wrapped in cling film to avoid peat oxidation and stored in the dark at 4 °C to minimise photo and biodegradation.

2.2 Sample processing

2.2.1 Bulk density and carbon storage

To determine the bulk density (BD), samples of 10 cm were taken every 50 cm down each peat column. These samples were then weighed, oven dried at 105 °C for 48 hours, and then re-weighed for dry weight. BD was calculated by: mass of dry peat (g) / volume (cm^3) (Tonks et al., 2017). The carbon stock (Mg ha^{-1}) was then calculated by multiplying the carbon per unit volume of soil (Cv) (BD multiplied by TOC) by the volume per layer (m^3 ha^{-1}) (depth per layer (m) multiplied by 1,000) (Agus et al., 2011).

2.2.2 ^{14}C dating and peat accumulation rates

Samples for were taken from the basal peat and at a point of change in peat texture and/or colour part way up the core at: 354-356 and 314-316 cm for *Rhizophora*; 438-440 and 234-236 cm for mixed forest, 507-509 (this date was not correct) and 234-236 cm for *Campnosperma* and 502-506 and 234-236 cm for *Cyperus*, and analysed by Beta Analytic for radiocarbon dating. Peat accumulation rates were calculated as in Phillips et al. (1997), with the depth to the surface or next date, divided by the peat age (BP).

2.2.3 Gas chromatography of saturated hydrocarbons

Differing carbon chain lengths of leaf wax *n*-alkanes are produced from different plant types, and can be used to recognise past vegetation types (Nichols et al., 2006). Short chain mainly odd numbered homologues, from C_{13}-C_{25} maximising at C_{15} or C_{17}, are mainly synthesized by aquatic algae and plankton; whereas long chain odd numbered homologues, C_{23}-C_{35} maximising at C_{29}, C_{31} or C_{33}, are often synthesized from vascular plants (Newell et al., 2016). It has also been suggested that even numbered mid-chain *n*-alkanes (C_{21}-C_{26}) may indicate decomposition which can lead to chain shortening (Schellekens and Buurman, 2011).

The following method is similar to that of Newell et al. (2016). Each core were sub-sampled at four depths for *n*-alkane analysis. Selected freeze dried 1 g samples were spiked with tetracosane-D50, squalene, hexatriacontane-D74 at 50 ng/µl, the samples were allowed to equilibrate. The samples were mixed with clean sand, copper powder and extracted dichloromethane/methanol (9:1 v/v) at 75 °C and 1200 psi using an ASE. The extracts were reduced to a smaller volume using a TurboVap, and hexane added to replace dichloromethane/methanol. Samples were then dried and hexane

added again for column chromatography. Alumina (aluminium oxide) was used in a column and was eluted with three-column volumes of *n*-hexane to isolate the saturate fraction. The eluent was reduced to 1 ml and reconstituted with *n*-hexane. A Hewlett Packard 6890 series GC-FID, fitted with an Agilent DB-1 ms UI column was used to analyse the saturates. The oven temperature was raised from 60 °C (isothermal for 1 min) to 320 °C (isothermal for 15 mins) at 10 °C min^{-1}. 1 µl was injected at 280°C in splitless mode for 0.7 min and subsequently split 1:10. Helium was used as a carrier gas (1 ml min^{-1}). The peak areas generated were integrated for the abundances of *n*-alkanes.

2.2.4 FTIR spectroscopy

Fourier Transform Infrared Spectroscopy (FTIR) can distinguish the composition of chemical classes due to the vibrational characteristics of their structural chemical bonds, within the organic matter (Artz et al., 2006; Artz et al., 2008; Vane et al., 2003). In this study FTIR was used to track decomposition through the peat profile due to the reduction in carbohydrates with depth, compared to aromatic compounds (Artz et al., 2006). Specifically, for the analysis five samples throughout the full depth of each core analysed but as the intensity of the relevant peak areas in the mineral layers were very low the paper only included data from the peat layers in each core.

Diamond attenuated total reflectance (DATR) FTIR spectroscopy was used to perform spectral characterisation of the peat samples, with the method similar to that of Artz et al. (2008). Freeze dried, powered samples were placed directly onto a DATR/KRS-5 crystal and pressed with a flat tip powder press to evenly distribute the sample. The spectra were acquired by averaging 128 scans at 4 m^{-1} resolution over the range 4000-550 $cm^{-1}$and corrected for background changes in water vapour and CO_2. The data

was normalised by subtraction of the sample minimum then division by the sample average. The 1030/1506 cm^{-1} ratio was used to identify peat humification, as this compares the relative intensities of carbohydrates (C-O stretch in cellulose) to aromatic peaks (aromatic ring stretching).

2.2.5 Rock-Eval6 pyrolysis

Rock-Eval pyrolysis is a technique which has been used recently to track bulk changes in organic matter composition and degree of decomposition (Disnar et al., 2003; Kemp et al., 2017; Newell et al., 2016). Sediments (2 cm^2) were sub-sampled at 10 cm intervals, with samples also taken before and after obvious changes in texture and/or colour in the peat stratigraphy. Freeze dried, powdered samples, were analysed using a Rock-Eval(6) analyser, configured in standard mode (Kemp et al., 2017; Newell et al., 2016). Pyrolysis was performed under an inert atmosphere of N_2, with an initial isothermal stage where the samples were heated at 200 °C for 3 minutes, before the oven temperature was raised to 650 °C at 25 °C min^{-1}. The amount of hydrocarbons released during pyrolysis was detected using a flame ionisation detector (FID), with CO and CO_2 measured using infrared detectors (IR). The residual carbon was then burnt in an oxidation oven, which increased from 300 to 850 °C at 20 °C min^{-1}, with the final temperature held for 5 minutes. Rock-Eval parameters were calculated by integration of the amounts of hydrocarbons (HC), CO and CO_2 produced during the thermal cracking of the OM, between well defined temperature limits. In this study we assessed the geochemistry of the peat using the following selected parameters:

- TOC (wt%) calculated from the sum of the carbon moieties (HC, CO and CO_2)

- T_{max} (°C) which corresponds to the temperature when the maximum amount of hydrocarbons were released during pyrolysis.
- HI (mg HC g^{-1} TOC) which is the amount of bound hydrocarbons released relative to the TOC
- OI (mg O_2 g^{-1} TOC) which corresponds to the quantity of oxygen released as CO and CO_2 relative to TOC.
- The labile, intermediate and persistent C pools (C_l, C_i, and C_p, respectively) which correspond to the deconvolution of S2 pyrograms into six Gaussian signals (F1-F6) and representing HC compounds pyrolysed below 360 °C (F1-F2), between 360-450 °C (F3) and above 450 °C (F4-F6) (Saenger et al. 2013). C_l, C_i, and C_p were calculated for 5 depths at each site, respectively.

2.3 Statistical Analysis

Statistical analysis was performed using GenStat 17th edition statistical analysis software. Mixed linear models using residual maximum likelihood (REML) was used to test for differences in the measured variables with depth. Regression analysis was used to assess the relationship between TOC and HI and between BD and carbon storage. To investigate the relationship between vegetation type, depth and peat physical and chemical properties Principle Component Analysis was used. Specifically we plotted the principal component scores and the latent vectors to assess which samples have comparable eigenvalues and which variables contributed to grouping/separation among vegetation types and depths.

3 Results

3.1 Bulk density, carbon stock and peat accumulation rates

The mean BD over all the sites was 0.07 ± 0.02 g cm^{-3}, BD was comparable in surface

peats (at ca 50 cm) across the four sites, and then showed variable depth trends among sites to ca. 1.2 m depth. Below this point BD tended to increase gradually with depth (depth effect: $F_{(1, 50)}$=28.93, P<0.001). As expected BD was a strong predictor of carbon storage (per layer, excluding mineral intervals at the base of the cores) ($F_{(1,44)}$=165.69, P<0.001, r^2=0.79; Figure 2 a, 3 and 4).

TOC was high through the peat profiles at the mixed, *Campnosperma* and *Cyperus* sites while TOC was generally lower at the *Rhizophora* site (Figure 3). TOC was lower in the peat surface layers compared to deeper down in the peat profile at all four sites (depth effect: $F_{(1, 224)}$=89.78, P<0.001). The base of the peat at each site had low TOC values due to mineral matter. For example, *Rhizophora* peat had shelly material at the base, which increased up to 413 cm as shown by the decrease in TOC from 15.5% to 3.9%, while the other three cores had silty and sandy horizons at the base, indicated by low TOC values (Figure 3).

Variations in peat depth, bulk density and TOC resulted in variable total carbon stocks for each phasic community (Figure 2 c). Mixed forest had the greatest total carbon stock (Mg C ha^{-1}) of 1884, followed by *Rhizophora*, 1771, then *Campnosperma,* 1694 and *Cyperus*, 1488. The average carbon stock for all sites was 1710 ± 83.4 Mg C ha^{-1}. The profile of carbon stock showed similar trends to that of BD, with higher carbon density in the lower parts of the peat profiles (depth effect: $F_{(1, 50)}$= 18.82, P<0.01; Figure 2 b).

Peat radiocarbon ages are listed in Table 1. The basal peat at the *Cyperus* site was the oldest while the *Rhizophora* basal peat was youngest, with an age of 2680 ± 30 and 1530 ± 30 years BP, respectively. These dates were used to estimate peat accumulation rates, which ranged between 2.1 and 2.6 mm yr^{-1} in the upper part of

the peat profile and 1.2 and 2.9 mm yr^{-1} in deeper peat layers. The long-term apparent rate of carbon accumulation decreased from the edge to the interior of the peatland, in agreement with the peat accumulation rates. Overall, the values ranged from 45.6 to 102.2 g C m^{-2} yr^{-1}, with the highest rates found in at the *Rhizophora* site and the lowest in the deeper peat layers at the *Cyperus* site. In line with the peat accumulation rates, carbon accumulation rates varied among the upper and lower part of the peat profiles.

3.2 *n*-alkane distributions

At all four phasic communities, surface peat was dominated by high molecular weight *n*-alkanes. Specifically *Rhizophora* surface peat was rich in C_{25}, C_{27} and C_{29} *n*-alkanes (Figure 4 a). This was consistent with surface material at the mixed forest, which contained high concentrations of C_{27} and C_{29}, with only low amounts of all other *n*-alkanes (Figure 4 b). The *Campnosperma* surface peat gave a bimodal *n*-alkane distribution, with maxima at C_{11}, as well as high values of *n*-alkanes C_{24} and C_{25} (Figure 4 c). Also the *Cyperus* site had maxima of C_{25} and C_{27} in the surface peat (Figure 4 d).

In the deeper peat layers which were analysed for *n*-alkane, *n*-alkane profiles differed more among sites (Figure 4 a-d). At the *Rhizophora* site, in the sampling depth just below 1 m the *n*-alkane distribution range from C_{10}-C_{26}, with maxima at C_{11}, C_{16} and C_{25}. However, in the deepest analysed peat layer (316-318cm depth) C_{27} was present again. At the mixed forest site the *n*-alkane signature at 66-64 cm depth ranged between C_{10} and C_{28} with a maxima at C_{24}. At 238-236 cm depth, there was bimodal distribution, with high concentrations of C_{15} and C_{29}. For the *Campnosperma* site at

278-276 cm depth the n-alkane distribution was dominated by high amounts of C_{23}, C_{25} and C_{27}. At 466-464 cm depth there was greater concentration of slightly longer chain homologues, with maximal peaks at C_{24} and C_{26}. The two deeper peat layers sampled at the *Cyperus* site was dominated by slightly shorter chain lengths than the surface layer: The peat at 34-36 cm depth was dominated by homologues of C_{23}, C_{24} and C_{25}, as well as C_{19}. Deeper down, between layer 172-174 cm and 320-322 cm there was a strong maximum of C_{19} and a secondary maximum at C_{24}.

The base of the cores at each sites was dominated by short chain *n*-alkanes with a dominance of even over odd numbered chain lengths. At the *Rhizophora* and mixed forest site the distribution ranged from C_{10}-C_{25} with maxima at C_{16}. At the *Campnosperma* site the base peat was dominated by short chain homologues C_{11}, C_{18} and C_{25}. The *Cyperus* site also showed *n*-alkane distributions dominated by lower homologues in the base of the core.

3.3 Functional organic chemistry (FTIR)

The FTIR spectra for the four sites showed similar distributions of organic functional groups (Figure 5). Broad peaks between 3339 and 3349 cm^{-1} were assigned to stretching of O-H groups in cellulose, xylans and lignin. The two small sharp peaks at around 2918 and 2850 cm^{-1} represent the asymmetric and symmetric stretching of C-H in $-CH_2-$, attributed to fats, waxes, lipids and lignin (Artz et al., 2008; Chefetz et al., 1996; Vane et al., 2003). The shoulder at around 1700 cm^{-1} is shown in mixed forest, *Camposperma* and *Cyperus* peat, and represents the stretching of C=O of COOH functional groups (Vane et al., 2001; Vane 2003). Two peaks at 1593-1597 and 1505-1507 cm^{-1} are associated with aromatic C=C stretching, found mainly in lignin and other aromatics (Artz et al., 2008; Gandois et al., 2012; Vane et al., 2003). The strong peak at around 1030 cm^{-1} is from the C-O stretch and O-H deformation of polysaccharidic structures such as cellulose, although it is also found in lignin (Artz et al., 2008; Gandois et al., 2012).

For mixed forest, *Campnosperma* and *Cyperus* peat, the carbohydrate/aromatic (1030/1506 cm^{-1}) ratio was highest in surface peat (depth effect: $F_{(4, 12.4)}=5.91$, $P<0.01$; Figure 6). For Rhizophora peat, the carbohydrate/aromatic ratio was higher at 1.2 m than at the surface. In the deepest layer sampled at this site at ca. 3.15 m the ration was lower than that of the two more superficial layer. The carbohydrate/aromatic ratio ranged between 1.8 and 4.8 in the surface peat but below ca. 1.5 m ratios showed a smaller range apart from at the *Rhizophora* site, which had a lower ratio at depth than the other sites.

3.4 Bulk Geochemistry (Rock-Eval)

3.4.1 T_{max}, HI and OI profiles

The T_{max} varied significantly with depth (depth effect: $F_{(1, 225)}$=11.21, P<0.001). In the surface peat T_{max} was ca. 350 °C at the three forested sites (Figure 3 a-c). At the *Rhizophora* site T_{max} declined to ca 300 °C between 0.5 and 2.0 m. Then T_{max} became more variable between 2 and 4 m depth, ranging between 306-352 °C, and below 4 m T_{max} reached 400 °C as the peat became shelly. T_{max} remained high and stable at the mixed and *Campnosperma* sites down to 1 m after which T_{max} declined and became more variable. Below ca. 3 m, T_{max} at the mixed forest site declined to just over 300 °C and remained low to the base of the core, while at the *Campnosperma* site the deepest layers of the peat profile had T_{max} of ca. 400 °C. The surface peat at the *Cyperus* site had much lower T_{max} (262 °C) than the other sites and the T_{max} remained lower (<300 °C) than at the other sites to ca. 1 m depth (Figure 3 d). Below 1 m T_{max} values became more comparable to those of intermediate depths from the *Campnosperma* site.

The HI was highest between ca 0.5 to 1 m at all sites, while surface peat had slightly lower HI (depth effect: $F_{(1, 225)}$=171.71, P<0.001; Figure 3 a-d). Below this peak HI then generally declined towards the base albeit at different rates among the sites. The peat OI was also highest at the surface and declined gradually with depth at all sites (depth effect: $F_{(1, 225)}$=5.56, P<0.05; Figure 3 a-d). In the peat dominated intervals (see peat core log in Figure 4), increasing HI was positively correlated to TOC for mixed forest and *Campnoperma* peat, ($F_{(1,43)}$=10.27, P=0.003, r^2=0.19; $F_{(1,50)}$=9.04, P=0.004, r^2=0.15, respectively; Figure 7 a) but not for *Rhizophora* and *Cyperus* peat, ($F_{(1,31)}$=1.55, P=0.222 r^2=0.05; $F_{(1,50)}$=1.23, P=0.272, r^2=0.02, respectively; Figure 7 a). Overall, *Rhizophora* peat contained thermally labile organic matter, with most of the

values ranging between 294-313 °C, whereas the other peat types were comprised of organic matter with slightly higher thermally labilities, which ranged from 304-347 °C, and thermally stable compounds, which ranged from 359-412 °C (Figure 7b). For mixed forest and *Campnosperma* peat, there was no significant difference in the TOC between thermally labile (up to 360 °C) and thermally stable (360 °C and above) peat ($F_{(1,43)}$=1.97, P=0.168; $F_{(1,50)}$=1.87, P=0.177, respectively). However, for *Cyperus* peat, the TOC was significantly higher for thermally stable peat, than thermally labile ($F_{(1,50)}$=8.43; P=0.005).

C_l, corresponding to the least thermostable pool was highest in *Rhizophora* surface peat, and decreased with depth across all sites (depth effect: $F_{(4,12)}$=5.09, P<0.05; Figure 8 a) with a minima of 15% at 525 cm for *Cyperus* peat. C_i, did not vary significantly with depth (depth effect: $F_{(4,12)}$=1.42, P>0.2; Figure 8 b). C_p, the most thermostable pool, generally increased with depth in all peats (depth effect: $F_{(4,12)}$=4.68, P<0.05; Figure 8 c). The most thermostable pool was at 525 cm for *Cyperus* peat. C_i was more variable but was generally higher at greater depths.

3.4.2 Multivariate comparison of different sites

The scores and loadings of principal components 1 (horizontal axis) and 2 (vertical axis) explained 40 and 15.5 % of the observed variation, (Fig. 9). *Rhizophora* samples and basal mineral layers were separated from intermediate peat layers at the *Cyperus*, *Campnosperma* and mixed forest sites (Fig 9 a) by (i) high BD and OI and low TOC and HI values and (ii) high concentrations of mid-chain length *n*-alkanes (C17, 20, 22 and 24) to the right (Fig 9 b). Surface samples were grouped in the upper-left part of Figure 8 a, and were characterised by high concentrations of

long chain n-alkanes (Figure 8 b). The long chain n-alkanes (C28-C31) correlated to the carbohydrate/aromatic ratio while the TOC and HI values correlated positively to C23, C25 and C26. T_{max} positively correlated to short chain *n*-alkanes (C13-14) (Figure 8b).

4 Discussion

4.1 Carbon stocks and long term carbon accumulation rates

The average carbon stock for all sites was 1710 ± 83.4 Mg C ha^{-1}, which is within the range of values reported for tropical peatlands elsewhere. Reported C stocks vary considerably among geographical areas, for example 2772 and 3130 Mg C ha^{-1} in undisturbed forested peatland sites in Indonesia (Page et al., 2006; Jaenicke et al., 2008), 1002 and 975 Mg C ha^{-1} in secondary peat swamp forest in Indonesia and Malaysia (Saragi et al., 2016; Tonks et al., 2017), and 892 and 1391 Mg C ha^{-1} in pristine forested peatlands the Amazon basin (Draper et al., 2014). The variation in C stocks (Figure 2 c) reported for the different communities highlights potential for spatial variability even over relatively short distances in response to different organic matter input and decomposition environments (Figure 3, 4 and 6), however, these within system differences were much smaller magnitude than the range reported across different regions. The higher C stocks at the *Rhizophora* and mixed forest sites, i.e. the two sites closest to the edge of the peatland, suggests that the common assumption of greater C stocks in later successional stages (Clymo 1984; Phillips et al., 1997) is too simplistic to be valid across large tropical peatlands. It also highlights

that *Rhizophora* forest store as much carbon as an equivalent area of freshwater peat swamp forest.

The greater bulk density and peat storage with depth at all sites corresponded with declining carbohydrate/aromatic ratios throughout the peat profile (Figure 2 and 6). This suggests a decrease in the proportion of coarse, hollow fibres in peat and a corresponding rise in smaller organic particle size with depth following decomposition, resulting in a closed peat structure with high carbon density (Huat et al., 2011). Peat accumulation rates were similar to those reported by Phillips et al. (1997). However, the rate for *Cyperus* peat reported by Phillips et al. (1997) was 5.6 mm yr^{-1}, which is greater than the rates we report for this community indicting either variation in ^{14}C dates or spatial variability in peat accumulation within phasic communities possibly associated with different accumulation rates in different parts of the peatland (Table 1).

The long-term apparent rate of carbon accumulation decreased from the *Rhizophora* to the *Cyperus* phasic community, which is in agreement with the peat accumulation rates and supports our first hypothesis, which predicted that carbon accumulation rate would vary with the phasic communities. The greater carbon accumulation rate in the *Rhizophora* forest may be linked to *Rhizophora* tissue being chemically resistant to decomposition and/or possibly rapid burial of litter material by marine clays, as indicated by the high bulk density and low C content (Figure 2 and 3) in the sediments found at this site, protect the organic matter from rapid microbial decay at the peat surface (Schmidt et al., 2011). Similar variation exists among Amazonian peat swamp forest types, where mixed palm swamp, *Mauritia flexuosa* palm swamp and open peatland had apparent carbon accumulation rates of 74, 39 and 85 g C m^{-2} yr^{-1}, respectively (Lähteenoja et al., 2009). Variable within site rates (i.e. with depth), in

line with those reported in our study, between 1.3 to 94.3 g C m^{-2} yr^{-1} were reported in Kalimantan, Indonesia (Page et al., 2004), reflecting contrasting organic matter input and loss rates over time.

4.2 Changes in peat chemistry with depth

n-alkane distributions

The abundance of long chain *n*-alkanes in surface peat clearly indicated terrestrial inputs, supporting our second hypothesis, which predicted that surface peat was poorly decomposed, with a high abundance of long chain *n*-alkanes (Figure 3). Specifically, there was a strong signature indicating terrestrial organic matter at all of our study sites, characterised by odd numbered long chain homologues (C_{25}-C_{27}) (Newell et al., 2016), for example from epicuticular waxes (Eglinton and Hamilton, 1967, Kristensen et al., 2008; Vane et al., 2014; Ranjan et al., 2015). The high relative abundance of odd numbered long chain *n*-alkanes in surface peats at our three forest sites is comparable to *n*-alkane distributions in surface samples from *Rhizophora* stands and mixed forest swamps in in the Florida Everglades, USA and Kalimantan, Indonesia, respectively, which were both dominated by a strong presence of C_{27}, C_{29} and C_{31} while the high abundance long change n-alkankes, especially C_{25} and C_{27}, at the Cyrerus site matches will surface sedge and phramecties peats from temeprate wetland sites (Dehmer, 1995).

The *n*-alkane distributions at depth partially supported our second hypothesis that enhanced decomposition with depth would correspond to greater concentrations of mid-chain length and even numbered *n*-alkanes in deeper peat layers (Schellekens and Buurman, 2011; Newell et al., 2016). Although this was the case in some

instances, e.g. greater abundance of both shortened mid-chain lengths and even numbered *n*-alkanes in deeper layers at the mixed forest, *Camponsperma*, and Cyperus sites, it was not a consistent trend of more mid-chain lengths with depth. Instead, the presence of long chain homologs at depth at both the *Rhizophora* and mixed forest sites suggests preservation of plant inputs due to low decomposition rates in some layers (Ranjan et al., 2015) and/or transport of freshly fallen leaf material by soil fauna, e.g. crabs, to deeper soil profiles (Kristensen 2008).

As expected, the basal peat at all sites had strong signatures of short chain *n*-alkanes, with an even over odd number chain length dominance, reflecting the marine base of the site (Phillips et al., 1997; Ranjan et al., 2015; Newell et al., 2016; Hoyos-Santiallan et al., 2016). However, the contribution of short chain *n*-alkanes throughout the peat profiles is intriguing, because it suggests strong bacterial/algae and plankton inputs to the peat (Ranjan et al., 2015; Witt et al., 2016) not only at the *Rhizophora* site by the coast, but also at the three sites further inland. We speculate that this reflects periods of very high water tables similar to the open marshy areas currently found at the central parts of the San San Pond Sak peat dome (Phillips et al., 1997; Wright et al., 2011).

Peat functional organic chemistry

The peat organic functional groups (Figure 4) were broadly comparable to those reported for mixed secondary peat swamp forests in Malaysia, although the carbohydrate/aromatic ratios reported here were lower (<5) compared to the study in Malaysia (approx. 12; Tonks et al., 2017). Furthermore, strong variation among peat swamp forest communities with regard to carbohydrates, as well as long chain fatty acids, was shown previously at the Panama site (Wright et al., 2011; Hoyos-Santillan et al., 2016). In line with our third hypothesis, which predicted decreasing carbohydrate

proportions with depth due to preferential decomposition of carbohydrates, the carbohydrate/aromatic ratio consistently declined with depth at three of the four sites, while at the *Rhizophora* site this decline was only evident below ca. 1 m (Figure) which may be linked to crabs transporting leaf material into their burrows as mentioned above. Increasing aromaticity and depletion of carbohydrates with depth, in the top 2 m, was reported previously for *Cyperus* and *Campnosperma* phasic communities (Wright et al., 2011). In parallel, depletion of long chain fatty acids (>C_{20}) around 0.5-1.5 m depth was reported for the mixed forest site (Hoyos et al., 2016). Together these findings suggest that irrespective of the functional group organic chemistry of the litter inputs, progression of peat decomposition and preferential decay of carbohydrates result in comparable carbohydrate/aromatic ratios across contrasting phasic communities. This may, in part, drive the relatively comparable BD and carbon storage in the different peat layers, as well as the LORCA (Figure 2, Table 1) between sites, despite contrasting litter inputs (Figure 3).

Bulk peat Rock-Eval

The low T_{max} and high HI index in the surface peat relative to the peat layer immediate below (Figure 3) is consistent with fresh litter inputs rich in carbohydrates, proteins and lipids (Disnar et al., 2003; Hetényi et al., 2006). The strong differences in T_{max} in the surface peat among the vegetation communities supported the first part of our fourth hypothesis, suggesting that litter inputs strongly affects the thermostability of the peat. The low T_{max} values found at the *Cyperus* site are most likely due to low lignin and higher carbohydrate content of grasses (Figure 6; Kemp et al., 2017; Vane et al., 2001; Nimz et al., 1981). The larger C_l pool at the *Rhizophora* site, despite higher T_{max} compared to the *Cyperus* site, might be linked to low molecular weight organic

compounds, for example because sugars are not included in the S2 signal (which is used for calculating the C pools) but are captured by the S1 signal (Carrie et al., 2012).

The increasing T_{max} and HI below the peat surface suggest rapid depletion of the most thermally labile compounds, leaving thermally stable compounds behind. Indeed, high HI values (> 300 mg HC g^{-1} TOC), in line with the HI values found in the top 0.5 to 2 m of peat in our study (although this varied among sites), are typically observed in plant tissues such as leaves and other material rich in polysaccharides with a high degree of hydrogenation and minimal transformation (Marchand et al., 2008). The decline in OI and HI with depth indicate SOM maturation and persistence of woody materials, which are richer in lignin, and have a high resistance to anaerobic decay (Disnar et al., 2003, Hetenyi et al., 2005, Saenger et al., 2013). At greater depth HI values continue to decrease, reflecting degraded plant material and increased humification of SOM, including greater aromaticity and dehydrogenation (Figure 3; Hetenyi et al., 2006, Carrie et al., 2012, Sebag et al., 2016). Increasing humification with depth is also supported by the depletion of carbohydrates down core, as demonstrated by the FTIR spectra and ratios (Figure 6), and the gradual decline in C_I and concurrent increase in C_P (Figure 8)

The relatively low T_{max} between ca. 0.5 and 2 m at the *Rhizophora* site is probably due to incorporation of a diverse mix of plant biopolymers and the addition of other organic matter inputs (e.g. bacteria), or a greater proportion of decayed remains as suggested by the higher abundance of short chain *n*-alkanes at intermediate depths at the *Rhizophora* site (Figure 4 a). In contrast, the high T_{max} values in the deeper shelly parts of the peat profile may be due to in-wash and incorporation of thermally stable re-worked marine organic matter. The highly variable T_{max} and changes in the relative sizes of the three carbon pools in the deeper parts of the three more interior sites,

particularly at the *Campnosperma* and *Cyperus* sites, indicates regular shifts in the thermostability of the organic matter due to shifts in the dominant vegetation inputs or changes in the decomposition environment, most likely related to water table fluctuations, which is a strong driver of decomposition in tropical peatlands (Couwenberg et al., 2010; Hoyos-Santillan et al., 2015). Taken together the low T_{max} in the surface peat supports our fourth hypothesis of greater T_{max} with depth. However, the strong shifts in T_{max} and thermostability throughout the peat profiles suggest that T_{max} reflects dynamic changes in the input and decomposition environment.

The increase in C_i and C_p pools with depth, broadly consistent in the *Rhizophora*, mixed forest and *Cyperus* sites, suggests that thermostability of stored carbon increases with depth. The decline in C_l between surface and subsurface samples indicates that there is relatively rapid initial degradation, but also that the process continues in the longer term as declines are generally consistent to depths of 5 m (Figure 8). The exception to this trend is the *Campnosperma* site, where there was a large increase in C_l at approximately 276 cm, matching changes in *n*-alkane distributions and T_{max} values with depth, supporting the notion of changes in organic matter input over time.

Conclusions

Carbon stocks were large but variable among the phasic communities, with the largest C stocks in mixed forest and the highest long-term apparent carbon accumulation rate at the *Rhizophora* site demonstrating that these sites are important C stores. Although the long-chain *n*-alkane signature in the surface peat indicate that this layer is mainly composed of poorly degraded terrestrial organic, the

variable carbohydrate to aromatics ratio suggest that the functional chemistry of the litter inputs differ considerably among sites, i.e. higher relative abundance of aromatic functional groups in the *Rhizophora* litter compared to the Cyperus site. Alternatively, more rapid loss of carbohydrates during the initial phases of decomposition at the *Rhizophora* site explains the lower carbohydrate to aromatic ratio at this site. Below the surface peat layers, progressing decomposition was indicated by an increase in mid-chain length *n*-alkanes at the *Cyperus* and the *Campnosperma* sites, however, this was not the case at the other two sites suggesting either preservation of the vegetation puts or redistribution of fresh litter inputs to deeper in the peat profile by for example soil fauna. The fact that the carbohydrate to aromatic ratios became not only lower but also more similar with depth (but slightly less so at the *Rhizophora* site) indicate that the decay processes gives similar end points irrespective of the contrasting surface peat chemistry as indicated by strong variation in both peat functional organic chemistry and thermolability. In line with the shifts toward more aromatic peat chemistry, the peat was more thermostabile with depth, which suggest initial rapid depletion of the labile pool followed by more gradual decomposition.

Taken together, it is clear that litter inputs strongly impact litter chemistry of the surface peat. However, as litter decay and the formed peat is affected by additional factors (e.g. sedimentation and soil fauna) the chemical signature of the original litter inputs are heavily modified. Our data suggest that although the quality of the fresh litter inputs (e.g. aromaticity) may explain initial decomposition rates and contribute to peat formation (Hoyos Santillan et al., 2016), ultimately the total carbon storage at

these sites is controlled by how variation in environmental conditions govern long term decay processes rather than litter inputs linked to specific vegetation types.

Acknowledgements

We thank Eric Brown for help in the field collecting the cores and Alexander Kim, Bill McNaughton and Vicky Moss-Hayes for their assistance in the laboratory. CHV publishes with the permission of the Executive Director of the British Geological Survey (NERC) .

5 References

Agus F, Hairiah K, Mulyani A. 2011. Measuring carbon stock in peat soils: practical guidelines. Bogor, Indonesia: World Agroforestry Centre (ICRAF) Southeast Asia Regional Program, Indonesian Centre for Agricultural Land Resources Research and Development. 60p

Anderson, J.A.R., 1964. The structure and development of the peat swamps of Sarawak and Brunei. The Journal of tropical geography, 18.

Andriesse, J.P., 1988. Nature and management of tropical peat soils (No. 59). Food & Agriculture Org.

Artz, R.R., Chapman, S.J. and Campbell, C.D., 2006. Substrate utilisation profiles of microbial communities in peat are depth dependent and correlate with whole soil FTIR profiles. Soil Biology and Biochemistry, 38(9), 2958-2962.

Artz, R.R., Chapman, S.J., Robertson, A.J., Potts, J.M., Laggoun-Défarge, F., Gogo, S., Comont, L., Disnar, J.R. and Francez, A.J., 2008. FTIR spectroscopy can be used as a screening tool for organic matter quality in regenerating cutover peatlands. Soil Biology and Biochemistry, 40(2), 515-527.

Biester, H., Knorr, K.H., Schellekens, J., Basler, A. and Hermanns, Y.M., 2014. Comparison of different methods to determine the degree of peat decomposition in peat bogs.

Brain, M.J., Kemp A.C., Hawkes A., Engelhart, S., Vane, C.H., Cahill, N., Hill, T.D., Engelhart, S., Donnelly, J., Horton, B.P. 2017. Exploring mechanisms of compaction in salt-marsh sediments using Common Era relative sea-level reconstructions. The contribution of mechanical compression and biodegradation to compaction of salt-marsh sediments and relative sea-level reconstructions. *Quaternary Science Reviews*167, 96-111.

Chefetz, B., Hatcher, P.G., Hadar, Y. and Chen, Y., 1996. Chemical and biological characterization of organic matter during composting of municipal solid waste. Journal of Environmental Quality, 25(4), 776-785.

Chimner, R.A. and Ewel, K.C., 2005. A tropical freshwater wetland: II. Production, decomposition, and peat formation. Wetlands Ecology and Management, 13(6), 671-684.

Clymo R.S., 1984. The Limits to Peat Bog Growth. Philosophical Transactions of the Royal Society of London. Series B, Biological Sciences, 303(1117), 605-654

Cohen, A.D., Raymond, R., Ramirez, A., Morales, Z. and Ponce, F., 1989. The Changuinola peat deposit of northwestern Panama: a tropical, back-barrier, peat (coal)-forming environment. International Journal of Coal Geology, 12(1-4), 157-192.

Dargie, G.C., Lewis, S.L., Lawson, I.T., Mitchard, E.T., Page, S.E., Bocko, Y.E. and Ifo, S.A., 2017. Age, extent and carbon storage of the central Congo Basin peatland complex. Nature.

Dehmer, J., 1995. Petrological and organic geochemical investigation of recent peats with known environments of deposition. International Journal of Coal Geology, 28(2-4), 111-138.

Disnar, J.R., Guillet, B., Kéravis, D., Di-Giovanni, C. and Sebag, D., 2003. Soil organic matter (SOM) characterization by Rock-Eval pyrolysis: scope and limitations. Organic geochemistry, 34(3), 327-343.

Disnar, J.R., Jacob, J., Morched-Issa, M., Lottier, N. and Arnaud, F., 2008. Assessment of peat quality by molecular and bulk geochemical analysis: Application to the Holocene record of the Chautagne marsh (Haute Savoie, France). Chemical geology, 254(1), 101-112.

Draper, F.C., Roucoux, K.H., Lawson, I.T., Mitchard, E.T., Coronado, E.N.H., Lähteenoja, O., Montenegro, L.T., Sandoval, E.V., Zaráte, R. and Baker, T.R., 2014. The distribution and amount of carbon in the largest peatland complex in Amazonia. Environmental Research Letters, 9(12), 124017.

Eglinton, G. and Hamilton, R.J., 1967. Leaf epicuticular waxes. Science, 156:1322-1335.

Engelhart, S.E., Horton, B.P, Nelson, A.R., Hawkes, A.D., Witter, R.C., Wang, K., Wang, P-.L., Vane, C.H., 2013. Testing the use of microfossils to reconstruct great earthquakes at Cascadia. Geology 41(10), 1067-1070.

Gandois, L., Cobb, A.R., Hei, I.C., Lim, L.B.L., Salim, K.A. and Harvey, C.F., 2013. Impact of deforestation on solid and dissolved organic matter characteristics of tropical peat forests: implications for carbon release. Biogeochemistry, 114(1-3), 183-199.

Hetényi, M., Nyilas, T., Sajgó, C. and Brukner-Wein, A., 2006. Heterogeneous organic matter from the surface horizon of a temperate zone marsh. Organic geochemistry, 37(12), 1931-1942.

Hobbie, S.E., Schimel, J.P., Trumbore, S.E. and Randerson, J.R., 2000. Controls over carbon storage and turnover in high-latitude soils. Global Change Biology, 6(S1), 196-210.

Hooijer, A., Page, S., Canadell, J.G., Silvius, M., Kwadijk, J., Wösten, H. and Jauhiainen, J., 2010. Current and future CO_2 emissions from drained peatlands in Southeast Asia. Biogeosciences, 7, 1505-1514.

Hoyos-Santillan, J., Lomax, B.H., Large, D., Turner, B.L., Boom, A., Lopez, O.R. and Sjögersten, S., 2015. Getting to the root of the problem: litter decomposition and peat formation in lowland Neotropical peatlands. Biogeochemistry, 126(1-2), 115-129.

Jaenicke, J., Rieley, J.O., Mott, C., Kimman, P. and Siegert, F., 2008. Determination of the amount of carbon stored in Indonesian peatlands. Geoderma, 147(3), 151-158.

Jansen, B., Nierop, K.G., Hageman, J.A., Cleef, A.M. and Verstraten, J.M., 2006. The straight-chain lipid biomarker composition of plant species responsible for the dominant biomass production along two altitudinal transects in the Ecuadorian Andes. Organic Geochemistry, 37(11), 1514-1536.

Kemp, A.C., Horton, B.P., Nikitina, D., Vane, C.H., Potapova, M., Weber-Bruya, E., Culver, S.J., Repkina, T. and Hill, D.F., 2017. The distribution and utility of sea-level indicators in Eurasian sub-Arctic salt marshes (White Sea, Russia). Boreas, 46(3), 562-584 Kristensen, E. 2008. Mangrove crabs as ecosystem engineers; with emphasis on sediment processesJournal of Sea Research 59 (2008) 30–43

Kristensen, E., Bouillon, S., Dittmar, T. and Marchand, C., 2008. Organic carbon dynamics in Rhizophora ecosystems: a review. Aquatic Botany, 89(2), 201-219.

Lähteenoja, O., Ruokolainen, K., Schulman, L. and Oinonen, M., 2009. Amazonian peatlands: an ignored C sink and potential source. Global Change Biology, 15(9), pp.2311-2320.

Laiho, R., 2006. Decomposition in peatlands: reconciling seemingly contrasting results on the impacts of lowered water levels. Soil Biology and Biochemistry, 38(8), 2011-2024.

Limpens, J., Berendse, F., Blodau, C., Canadell, J.G., Freeman, C., Holden, J., Roulet, N., Rydin, H. and Schaepman-Strub, G., 2008. Peatlands and the carbon cycle: from local processes to global implications–a synthesis. Biogeosciences, 5(5), 1475-1491.

Marchand, C., Lallier-Verges, E., Disnar, J.R. and Kéravis, D., 2008. Organic carbon sources and transformations in Rhizophora sediments: a Rock-Eval pyrolysis approach. Organic Geochemistry, 39(4), 408-421.

Meyers, P.A., 2003. Applications of organic geochemistry to paleolimnological reconstructions: a summary of examples from the Laurentian Great Lakes. Organic geochemistry, 34(2), 261-289.

Minasny, B., Setiawan, B.I., Arif, C., Saptomo, S.K. and Chadirin, Y., 2016. Digital mapping for cost-effective and accurate prediction of the depth and carbon stocks in Indonesian peatlands. Geoderma, 272, 20-31.

Murdiyarso, D., Donato, D., Kauffman, J.B., Kurnianto, S., Stidham, M. and Kanninen, M., 2010. Carbon storage in Rhizophora and peatland ecosystems: a preliminary account from plots in Indonesia (No. CIFOR Working Paper no. 48, p. 35p). Center for International Forestry Research (CIFOR), Bogor, Indonesia.

Neuzil, S.G., 1997. Onset and rate of peat and carbon accumulation in four domed ombrogenous peat deposits, Indonesia. Biodiversity and Sustainability of Tropical peatlands, 55-72.

Newell, A.J., Vane, C.H., Sorensen, J.P., Moss-Hayes, V. and Gooddy, D.C., 2016. Long-term Holocene groundwater fluctuations in a chalk catchment: evidence from Rock-Eval pyrolysis of riparian peats. Hydrological Processes, 30(24), 4556-4567.

Nichols, J.E., Booth, R.K., Jackson, S.T., Pendall, E.G. and Huang, Y., 2006. Paleohydrologic reconstruction based on n-alkane distributions in ombrotrophic peat. Organic Geochemistry, 37(11), 1505-1513.

Nikitina, D.L., Kemp, A.C., Horton, B.P., Vane, C.H., van de Plassche, O. and Engelhart, S.E., 2014. Storm erosion during the past 2000 years along the north shore of Delaware Bay, USA. Geomorphology, 208, 160-172.

Nimz, H.H., Robert, D., Faix, O, Nemer, M., 1981. Carbon-13 NMR spectra of lignins:Structural differences between lignins in hardwoods, softwoods and grasses and compression wood. Holzforschung, 35, 16-26.

Page, S.E., Rieley, J.O. and Banks, C.J., 2011. Global and regional importance of the tropical peatland carbon pool. Global Change Biology, 17(2), 798-818.

Page, S.E., Rieley, J.O. and Wüst, R., 2006. Lowland tropical peatlands of Southeast Asia. Developments in Earth Surface Processes, 9, 145-172.

Page, S.E., Rieley, J.O., Shotyk, Ø.W. and Weiss, D., 1999. Interdependence of peat and vegetation in a tropical peat swamp forest. Philosophical Transactions of the Royal Society of London B: Biological Sciences, 354(1391), 1885-1897.

Page, S.E., Wűst, R.A.J., Weiss, D., Rieley, J.O., Shotyk, W. and Limin, S.H., 2004. A record of Late Pleistocene and Holocene carbon accumulation and climate change from an equatorial peat bog (Kalimantan, Indonesia): implications for past, present and future carbon dynamics. Journal of Quaternary Science, 19(7), 625-635.

Phillips, S., Rouse, G.E. and Bustin, R.M., 1997. Vegetation zones and diagnostic pollen profiles of a coastal peat swamp, Bocas del Toro, Panama.Palaeogeography, Palaeoclimatology, Palaeoecology, 128(1), 301-338.

Ranjan, R.K., Routh, J., Klump, J.V. and Ramanathan, A.L., 2015. Sediment biomarker profiles trace organic matter input in the Pichavaram Rhizophora complex, southeastern India. Marine Chemistry, 171, 44-57.

Rieley, J.O., Sieffermann, R. G. and Page, S. E.1992. The origin, development, present status and importance of the lowland peat swamp forests of Borneo. Suo, 43, 241-244.

Saenger, A., Cécillon, L., Sebag, D. and Brun, J.J., 2013. Soil organic carbon quantity, chemistry and thermal stability in a mountainous landscape: a Rock–Eval pyrolysis survey. Organic Geochemistry, 54, 101-114.

Saragi, M.F., Murdiyarso, D. and Sasmito, S.D., A preliminary assessment of carbon storage and productivity of peat swamp forest in Katingan, Central Kalimantan, Indonesia.

Schellekens, J. and Buurman, P., 2011. n-Alkane distributions as palaeoclimatic proxies in ombrotrophic peat: the role of decomposition and dominant vegetation. Geoderma, 164(3), 112-121.

Schmidt, M.W.I., Torn, M.S., Abiven, S., Dittmar, T., Guggenberger, G., Janssens, I.A., Kleber, M., Koegel-Knabner, I., Lehmann, J., Manning, D.A.C., Nannipieri, P., Rasse, D.P., Weiner, S. and Trumbore S.E., 2011. Persistence of soil organic matter as an ecosystem property. Nature, 478 (2011), pp. 49-56

Shimada, S., Takahashi, H., Haraguchi, A. and Kaneko, M., 2001. The carbon content characteristics of tropical peats in Central Kalimantan, Indonesia: estimating their spatial variability in density. Biogeochemistry, 53(3), 249-267.

Sjögersten, S., Cheesman, A.W., Lopez, O. and Turner, B.L., 2011. Biogeochemical processes along a nutrient gradient in a tropical ombrotrophic peatland. Biogeochemistry, 104(1-3), 147-163.

Sjögersten, S., Black, C.R., Evers, S., Hoyos-Santillan, J., Wright, E.L. and Turner, B.L., 2014. Tropical wetlands: A missing link in the global carbon cycle?. Global biogeochemical cycles, 28(12), 1371-1386.

Tonks, A.J., Aplin, P., Beriro, D.J., Cooper, H., Evers, S., Vane, C.H. and Sjögersten, S., 2017. Impacts of conversion of tropical peat swamp forest to oil palm plantation on peat organic chemistry, physical properties and carbon stocks. Geoderma, 289, 36-45.

Vane, C.H., 2003. Monitoring decay of black gum wood (*Nyssa sylvatica*) during growth of the shiitake mushroom (*Lentinula edodes*) using diffuse reflectance infrared spectroscopy. Applied spectroscopy, 57, 514-517.

Vane, C.H., Kim, A.W., Cave, M.R., Li, N. 2014. Equal abundance of odd and even *n*-alkanes from cycad leaves: Can the carbon preference index (CPI) faithfully record terrerstrial organic matter input at low latitudes. Encepharlatos 118, 10-12.

Vane, C.H**.,** Kim, A.W., Moss-Hayes V, Snape C.E, Castro-Diaz, M., Khan, N.S., Engelhart S.E. and Horton, B.P. 2013. Mangrove tissue decay by arboreal termites (Nasutitermes acajutlae) and their role in the mangrove C cycle (Puerto Rico): Chemical characterisation and organic matter provenance using bulk $\delta^{13}C$, C/N, alkaline CuO oxidation-GC/MS and solid-state ^{13}C NMR. Geochemsistry, Geophysics, Geosystems 14, 3176-3191.

Vane, C.H., Martin, S.C, Snape, C.E., Abbott, G.D. 2001. Degradation of lignin in wheat straw during growth of the Oyster mushroom (*Pleurotus ostreatus*) using off-line thermochemolysis with tetramethylammonium hydroxide and solid state ^{13}C NMR. Journal of Agriculture and Food Chemistry, 49, 2709-2716.

Vane, C.H., Rawlins, B.G., Kim, A.W., Moss-Hayes, V., Kendrick, C.P. and Leng, M.J., 2013. Sedimentary transport and fate of polycyclic aromatic hydrocarbons (PAH) from managed burning of moorland vegetation on a blanket peat, South Yorkshire, UK. Science of the total environment, 449, 81-94.

Wang, N., Zong, Y., Brodie, C.R. and Zheng, Z., 2014. An examination of the fidelity of n-alkanes as a palaeoclimate proxy from sediments of Palaeolake Tianyang, South China. Quaternary International, 333, 100-109.

Ward, S.E., Orwin, K.H., Ostle, N.J., Briones, M.J., Thomson, B.C., Griffiths, R.I., Oakley, S., Quirk, H. and Bardgett, R.D., 2015. Vegetation exerts a greater control on litter decomposition than climate warming in peatlands. Ecology, 96(1), 113-123.

Warren, M.W., Kauffman, J.B., Murdiyarso, D., Anshari, G., Hergoualc'h, K., Kurnianto, S., Purbopuspito, J., Gusmayanti, E., Afifudin, M., Rahajoe, J. and Alhamd, L., 2012. A cost-efficient method to assess carbon stocks in tropical peat soil. Biogeosciences, 9.

Weiss, D., Shotyk, W., Rieley, J., Page, S., Gloor, M., Reese, S. and Martinez-Cortizas, A., 2002. The geochemistry of major and selected trace elements in a forested peat bog, Kalimantan, SE Asia, and its implications for past atmospheric dust deposition. Geochimica et Cosmochimica Acta, 66(13), 2307-2323.

Witt, R., Günther, F., Lauterbach, S., Kasper, T., Mäusbacher, R., Yao, T. and Gleixner, G., 2016. Biogeochemical evidence for freshwater periods during the Last Glacial Maximum recorded in lake sediments from Nam Co, south-central Tibetan Plateau. Journal of Paleolimnology, 55(1), 67-82.

Wösten, J.H.M., Clymans, E., Page, S.E., Rieley, J.O. and Limin, S.H., 2008. Peat–water interrelationships in a tropical peatland ecosystem in Southeast Asia. Catena, 73(2), 212-224.

Wright, E.L., Black, C.R., Cheesman, A.W., Drage, T., Large, D., Turner, B.L. and Sjoegersten, S., 2011. Contribution of subsurface peat to CO2 and CH4 fluxes in a neotropical peatland. Global Change Biology, 17(9), 2867-2881.

Figure captions

Figure 1 Map of San San Pond Sak wetland, Panama.

The locations of the four sampling sites shown are: *Rhizophora* forest (*Rhizophora mangle*): 9°22'47.6"N, 82°22'06.0"W; mixed forest swamp: 9°23'07.1"N, 82°22'17.8"W; *Campnosperma panamensis* forest swamp: 9°23'16.3"N, 82°22'7.1"W and *Cyperus* 9°23'39.70"N, 82°21'58.33"W.

Figure 2 Depth profiles for: a) bulk density (BD) and b) carbon storage, for the four vegetation types. c) total carbon storage for the four vegetation types. All data excludes basal shelly and sandy intervals.

Figure 3 Visual down core log and down profile changes using Rock-Eval pyrolysis for: a) *Rhizophora*, b) Mixed Forest, c) *Campnosperma* and d) *Cyperus* sites. Samples for n-alkanes (data shown in Figure 4) were analysed from the following layers at the different sites *Rhizophora*: 0-2 cm, 116-118 cm, 316-318 cm, and 616-618 cm*,* Mixed Forest: 0-2 cm, 64-66 cm, 236-238 cm, 507-509 cm, *Campnosperma*: 15-17 cm, 276-278 cm, 464-466 cm, 527-529 cm, *Cyperus* 0-2 cm, 36-38 cm, 320-322 cm, 525-529 cm.

Figure 4 Changes in *n*-alkane abundances (ng g^{-1}) with depth for a) *Rhizophora*, b) mixed forest, c) *Campnosperma* and d) *Cyperus*. Higher *n*-alkane lengths indicate more terrestrial organic matter, lower *n*-alkane lengths indicate organic matter from aquatic origin.

Figure 5 Illustrative example of FTIR absorbance spectra, for *Cyperus* peat. Spectra were stacked and normalised (see text). Characteristic FTIR absorption bands are labelled.

Figure 6 Profiles of carbohydrate (average of 1029-1031 cm^{-1}) to aromatic (average of 1505-1507 cm^{-1}) ratios through the peat cores. The data is from peat only, i.e. excludes basal shelly and sandy intervals. Samples for n-alkanes (data shown in Figure 4) were analysed from the following layers at the different sites *Rhizophora*: 0-2 cm, 116-118 cm, 316-318 cm, and 616-618 cm, Mixed Forest: 0-2 cm, 64-66 cm, 236-238 cm, 507-509 cm, *Campnosperma*: 15-17 cm, 276-278 cm, 464-466 cm, 527-529 cm, *Cyperus* 0-2 cm, 36-38 cm, 320-322 cm, 525-529 cm.

Figure 3 Relationships between a) HI and TOC; b) T_{max} and TOC. The data is from peat only layer, i.e. excludes basal shelly and sandy intervals.

Figure 8 Changes in relative carbon pool size with depth for a) C_l, b) C_i, c) C_p pools in *Rhizophora*, Mixed forest, *Campnoserpma* and *Cyperus* stands.

Figure 9 a) Principal component scores for PC 1 and PC 2 for samples from the four different vegetation types, sampling depth is indicated in (m) by the side of each

symbol and b) Latent vector loadings for PC 1 and PC 2, n-alkanes are indicated in grey, all other parameters are shown in black.

Table 1. Radiocarbon ages, peat and carbon accumulation rates through the peat profiles at the four different sites. Dates 2, 4 and 7 correspond to the approximate earliest point of peat accumulation.

No.	Site	Depth Interval (cm)	Age ^{14}C yr BP	Peat accumulation rate* (mm yr-1)	Carbon accumulation rate* (mm yr-1)
1	*Rhizophora*	314-316	1190 +/- 30	2.6	102.2
2	*Rhizophora*	354-356	1530 +/- 30	1.2	62.9
3	Mixed forest	234-236	1200 +/- 30	2	56.5
4	Mixed forest	438-440	1920 +/- 30	2.9	91.9
5	*Campnosperma*	234-236	1000 +/- 30	2.3	61.5
6	*Cyperus*	234-236	1120 +/- 30	2.1	45.6
7	*Cyperus*	502-506	2680 +/- 30	1.7	48.4

*Peat and carbon accumulation rate are calculated up to the next know dates towards the surface, or, to the present (surface) date.

Figure 1

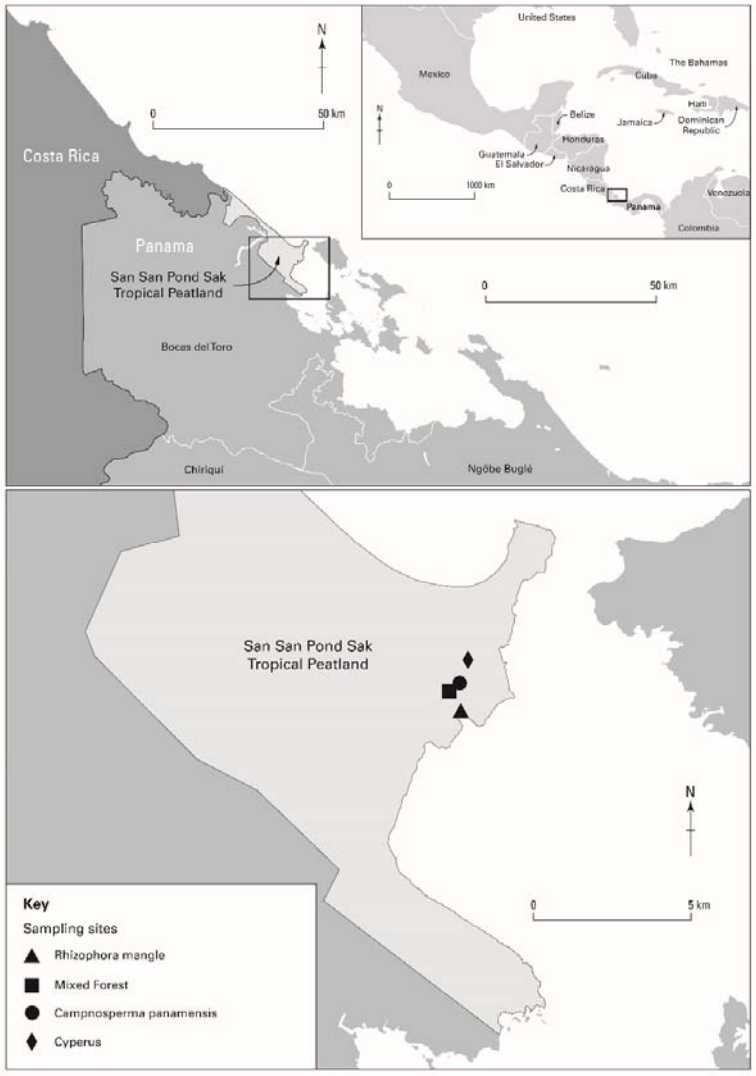
United States
Mexico
The Bahamas
Cuba
Haiti
Belize
Jamaica
Dominican Republic
Honduras
Guatemala
El Salvador
Nicaragua
Costa Rica
Panama
Venezuela
Colombia
1000 km
N
0
50 km
Costa Rica
Panama
San San Pond Sak Tropical Peatland
Bocas del Toro
Chiriqui
Ngöbe Buglé
San San Pond Sak Tropical Peatland
5 km
Key
Sampling sites
Rhizophora mangle
Mixed Forest
Campnosperma panamensis
Cyperus

Figure 2

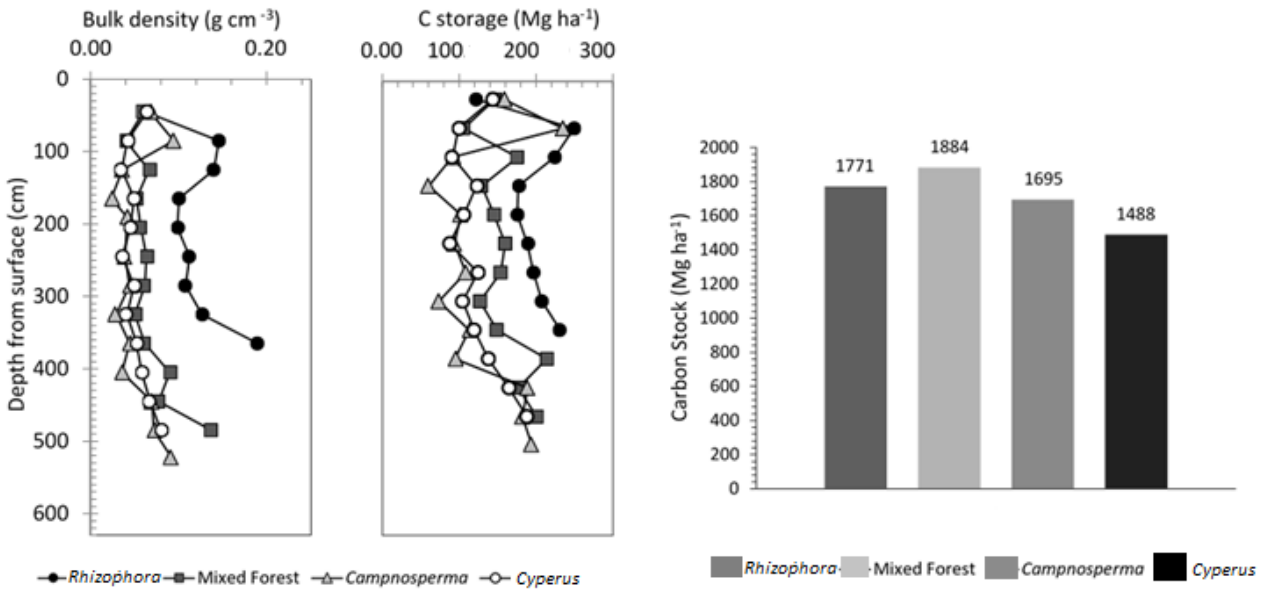
Bulk density (g cm -3)
0.00
0.20
C storage (Mg ha-1)
0.00
100
200
300
0
100
200
300
400
500
600
Depth from surface (cm)
Rhizophora
Mixed Forest
Campnosperma
Cyperus
Carbon Stock (Mg ha-1)
2000
1800
1600
1400
1200
1000
800
600
400
200
0
1771
1884
1695
1488
Rhizophora
Mixed Forest
Campnosperma
Cyperus

Figure 3

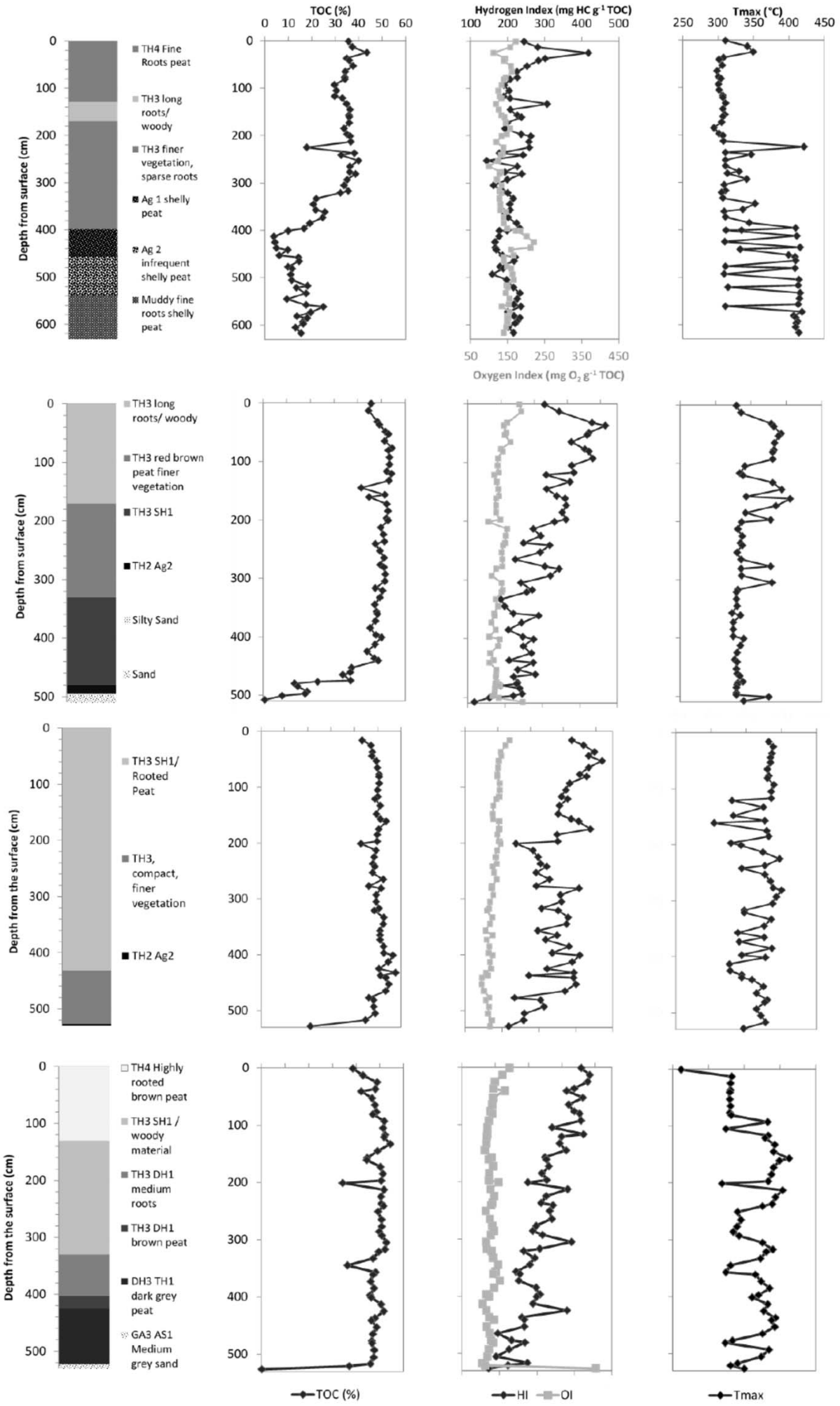
TOC (%)
Hydrogen Index (mg HC g-1 TOC)
Tmax (°C)
Oxygen Index (mg O2 g-1 TOC)
Depth from surface (cm)
TH4 Fine Roots peat
TH3 long roots/ woody
TH3 finer vegetation, sparse roots
Ag 1 shelly peat
Ag 2 infrequent shelly peat
Muddy fine roots shelly peat
TH3 long roots/ woody
TH3 red brown peat finer vegetation
TH3 SH1
TH2 Ag2
Silty Sand
Sand
Depth from the surface (cm)
TH3 SH1/ Rooted Peat
TH3, compact, finer vegetation
TH2 Ag2
TH4 Highly rooted brown peat
TH3 SH1 / woody material
TH3 DH1 medium roots
TH3 DH1 brown peat
DH3 TH1 dark grey peat
GA3 AS1 Medium grey sand
TOC (%)
HI
OI
Tmax

Figure 4

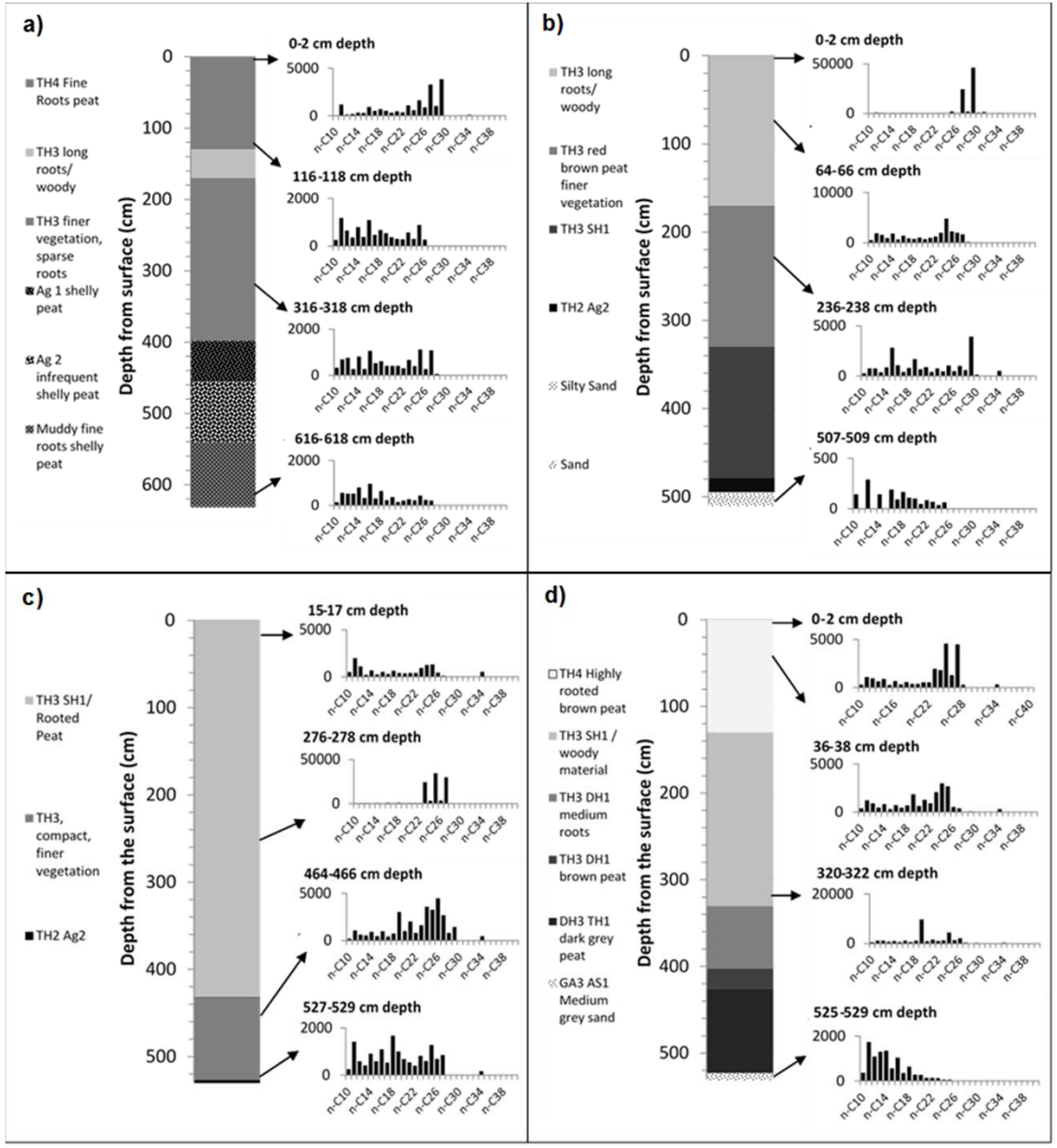
a)
TH4 Fine Roots peat
TH3 long roots/ woody
TH3 finer vegetation, sparse roots
Ag 1 shelly peat
Ag 2 infrequent shelly peat
Muddy fine roots shelly peat
Depth from surface (cm)
0-2 cm depth
116-118 cm depth
316-318 cm depth
616-618 cm depth
b)
TH3 long roots/ woody
TH3 red brown peat finer vegetation
TH3 SH1
TH2 Ag2
Silty Sand
Sand
Depth from surface (cm)
0-2 cm depth
64-66 cm depth
236-238 cm depth
507-509 cm depth
c)
TH3 SH1/ Rooted Peat
TH3, compact, finer vegetation
TH2 Ag2
Depth from the surface (cm)
15-17 cm depth
276-278 cm depth
464-466 cm depth
527-529 cm depth
d)
TH4 Highly rooted brown peat
TH3 SH1 / woody material
TH3 DH1 medium roots
TH3 DH1 brown peat
DH3 TH1 dark grey peat
GA3 AS1 Medium grey sand
Depth from the surface (cm)
0-2 cm depth
36-38 cm depth
320-322 cm depth
525-529 cm depth

Figure 5

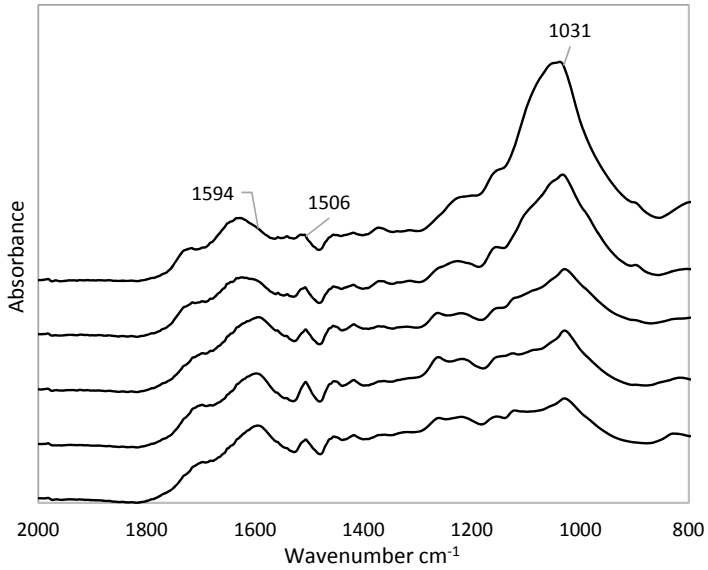
1031
1594
1506
Absorbance
2000
1800
1600
1400
1200
1000
800
Wavenumber cm-1

Figure 6

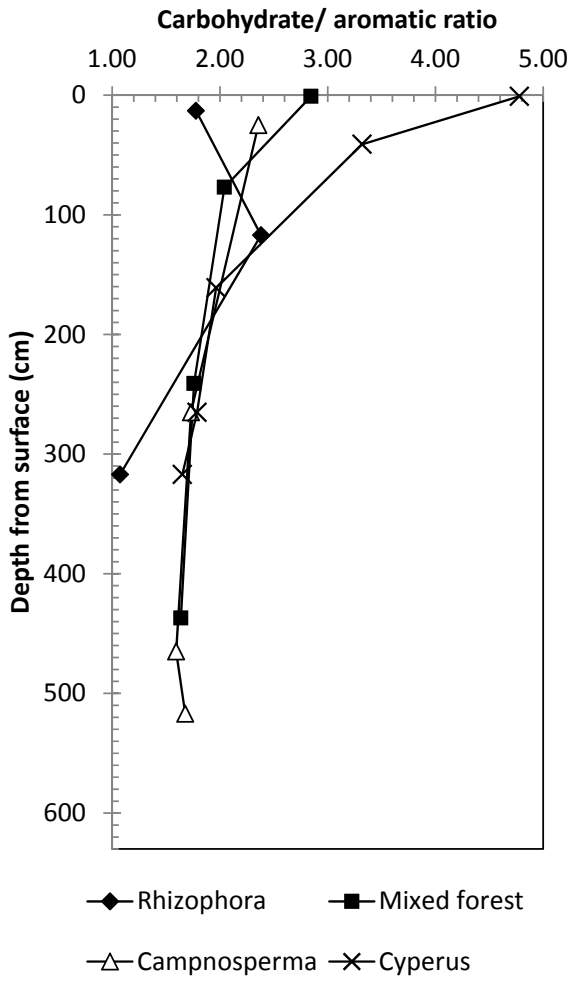
Carbohydrate/ aromatic ratio
1.00
2.00
3.00
4.00
5.00
0
100
200
300
400
500
600
Depth from surface (cm)
Rhizophora
Mixed forest
Campnosperma
Cyperus

Figure 7

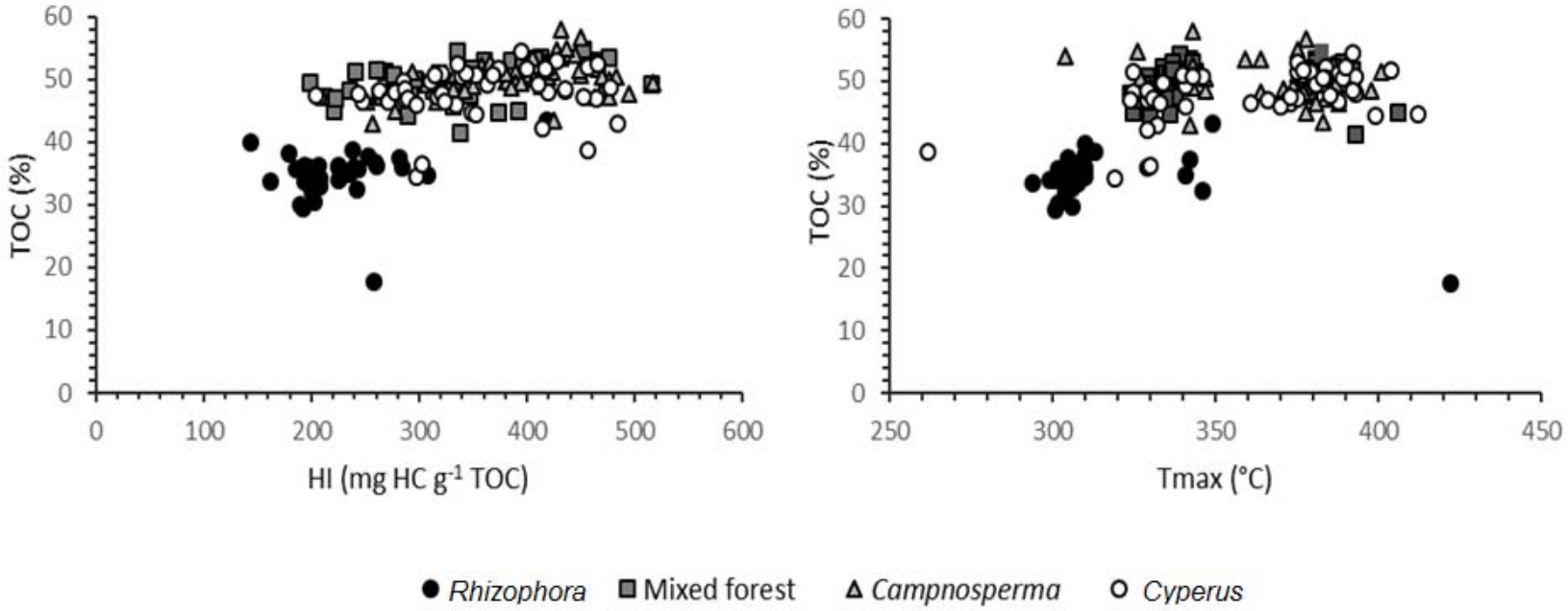
TOC (%)
HI (mg HC g-1 TOC)
Tmax (°C)
Rhizophora
Mixed forest
Campnosperma
Cyperus

Figure 8

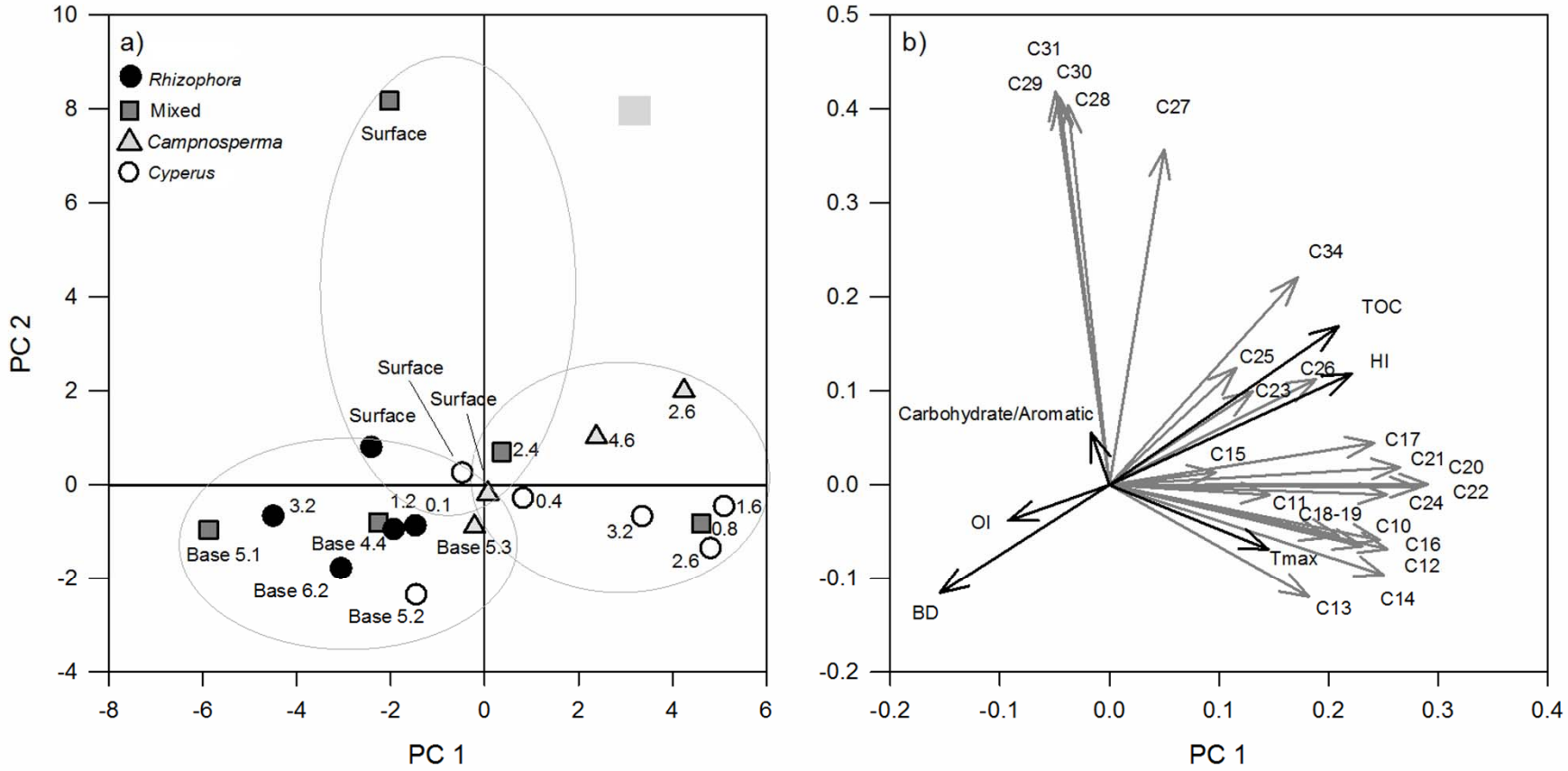
a)
Rhizophora
Mixed
Campnosperma
Cyperus
Surface
Surface
Surface
Surface
2.4
4.6
2.6
3.2
1.2
0.1
0.4
1.6
3.2
0.8
2.6
Base 5.1
Base 4.4
Base 5.3
Base 6.2
Base 5.2
PC 1
PC 2
b)
C31
C30
C29
C28
C27
C34
TOC
HI
C25
C26
C23
Carbohydrate/Aromatic
C17
C15
C21
C20
C22
C24
C11
C18-19
C10
C16
C12
OI
Tmax
C13
C14
BD
PC 1

Figure 9

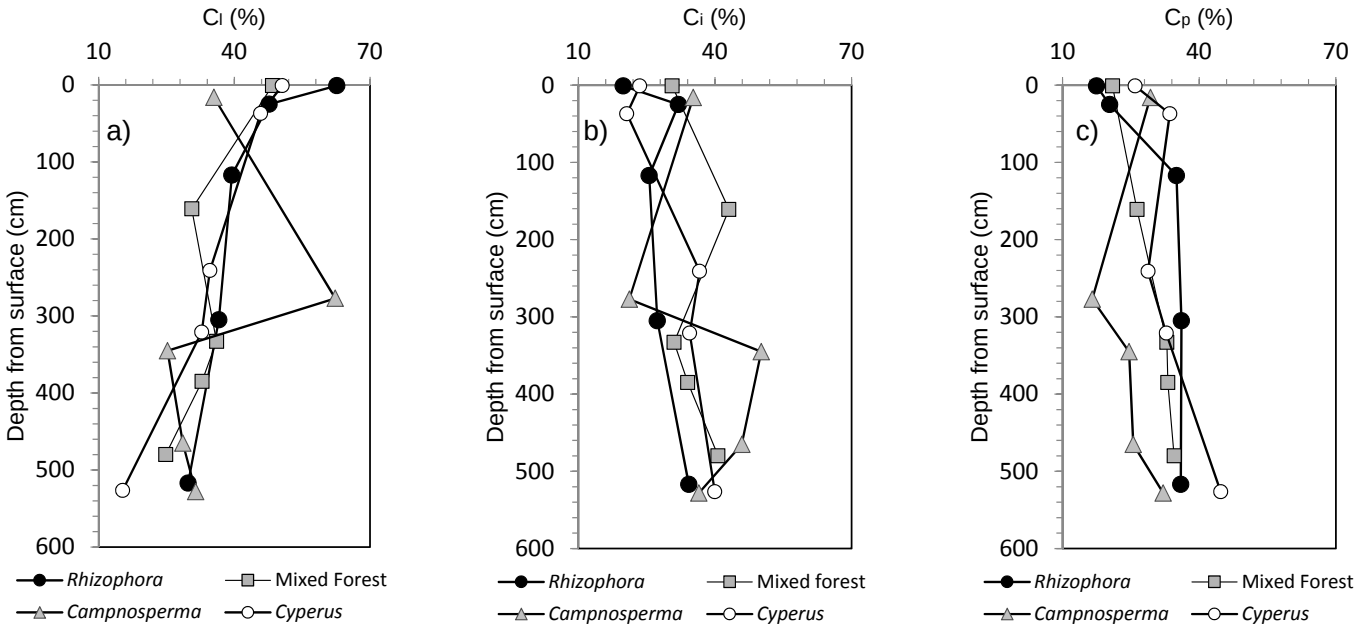
Cl (%)
10
40
70
0
100
200
300
400
500
600
Depth from surface (cm)
a)
Rhizophora
Mixed Forest
Campnosperma
Cyperus
Ci (%)
b)
Rhizophora
Mixed forest
Campnosperma
Cyperus
Cp (%)
c)
Rhizophora
Mixed Forest
Campnosperma
Cyperus